

Acoustic Instrumentation for Imaging and Quantifying Hydrothermal Flow in the NEPTUNE Canada Regional Cabled Observatory at Main Endeavour Field

*Russ Light and Vern Miller, APL-UW
Peter Rona and Karen Bemis, Rutgers University*

Program Description: Science and Engineering

The National Science Foundation Oceanographic Technology and Interdisciplinary Coordination (OTIC) program funded the engineering development and connection of the sonar instrument package to the Endeavor node of the NEPTUNE Canada Stage 1 component of the Regional Cabled Observatory (RCO) in the Main Endeavour Field (MEF) on the northern Juan de Fuca Ridge as part of the Ocean Observatories Initiative (OOI, Figure 1). The backbone cable of the NEPTUNE Canada RCO in the MEF was installed in 2007, the node was installed in 2008, and the observatory began operation in 2009. The sonar system will monitor seafloor hydrothermal flow using innovative acoustic imaging methods to provide time series measurements of changing geometry (size, shape, orientation, expansion rate, entrainment rate) and discharge (flow rate and volume flux) of buoyant hydrothermal plumes of black smokers venting from mineralized chimneys.

The sonar concurrently images the areal distribution of diffuse flow discharging from the surrounding seafloor on a spatial scale of a vent cluster (tens of meters). Connection to the cable provides the power and bandwidth to extend our present acoustic imaging capability (days to weeks on ROV or batteries) to months to years. This extension opens a new temporal domain to understand how hydrothermal flows and fluxes change with time and respond to external forcing by oceanic (tides and possibly hitherto undetected phenomena) and geologic (earthquakes, volcanic activity) processes on time scales ranging from hours to years and for elucidation of these processes through their linkages to the flow.

The system provides a near real-time, user-friendly data product for the community (3D images of buoyant plumes) and has automated signal processing for the large data acquisition rates anticipated. We apply our proven methods to measure 3D geometry, flow rate and volume flux of buoyant plumes and areal distribution of diffuse flow on the scale of a vent cluster (tens of meters).

Hydrothermal plumes and diffuse flow are driven by magmatic heat sources at ocean ridges and are agents of dispersal of heat and matter (inorganic elements and organic matter including microbes and larvae) transferred from the lithosphere into the ocean by sub-seafloor hydrothermal convection systems in quantitatively significant amounts (*Jenkins et al.*, 1978; *Edmond et al.*, 1979; *Mullineaux et al.*, 1991; *Kim et al.*, 1994; *Elderfield and Schultz*, 1996). High-temperature solutions (200° to 400°C) discharge as plumes with stems and caps from vents at mineralized chimneys. The plume stem comprises momentum driven jets at the source vents, which become buoyant plumes within the initial meters of rise. The buoyant plumes may rise up to hundreds of meters above the vents as a consequence of total weight deficiency per unit time (buoyancy flux) produced by the volume of lower density fluids (*Morton et al.*, 1956). As the buoyant plume rises, it entrains seawater until it attains neutral buoyancy relative to the density stratification of the surrounding ocean where the plume spreads laterally as a cap on the stem (*Morton et al.*, 1956; *Turner*, 1986). Plumes are generally bent by cross flow of deep ocean currents, which may reverse on a diurnal or semi-diurnal schedule when driven by tidal cycles.

Diffuse flow is the disseminated discharge of lower-temperature hydrothermal solutions (to tens of degrees C) through areas of the seafloor where the flow generally forms a patchy layer within

meters of the seafloor. The layer is laterally advected by prevailing currents and entrained in the updraft of black smoker plumes in varying proportions (McDuff, 1995; Stahr et al.; Johnson and Pruis, 2003; Pruis and Johnson, 2004; Viers et al., 2006; Garcia-Berdeal et al., 2006a,b). Quantitative assessment of diffuse flow in hydrothermal fields is important because the cumulative thermal and chemical flux through areas of the seafloor may equal or exceed that of focused flow from associated smokers (Rona and Trivett, 1992; Schultz et al., 1992). However, fluxes from diffuse flow are elusive to map with conventional methods because it occurs in irregular areas, fluids are clear lacking suspended particulate matter detectable by measuring absorption or backscatter of light and sound. The fortuitous snapshots of hydrothermal discharge that we make on our short cruises largely miss the variability of hydrothermal discharge, the interaction of the flow with the dynamic ocean, with living ecosystems, and the response of the flow to oceanic and geologic processes and events.

Models of the effects of tidal loading on seafloor hydrothermal systems predict that perturbations of outflow temperature will be small ($<0.1^{\circ}\text{C}$) and that of fluid velocity will be relatively large (Crone and Wilcock, 2005). We will quantify hydrothermal flow (plumes and diffuse flow) on time and space scales that respond to these interactions with our acoustic imaging instrumentation on the NEPTUNE Canada node at the Main Endeavour Field (MEF). For example, on the short-term end of the time scale (hours to weeks), our 23-hour time series of hourly acoustic images of a major plume rising from Grotto vent in the MEF shows the plume alternately bending NE and SW in response to forcing by current reversal in a mixed semi-diurnal tidal cycle (Rona et al., 2006).

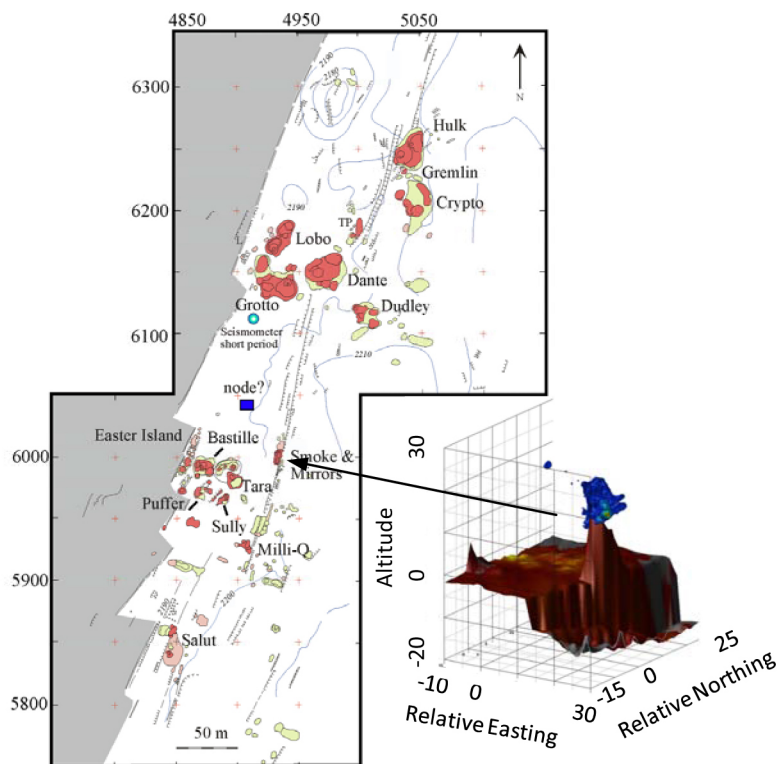


Figure 1. Left panel: Map of Main Endeavour Field (UTM coordinates in meters) showing approximate central position of NEPTUNE Canada node (small square near center) scheduled for installation in 2008. Right panel: Our acoustic image of lower portion of buoyant plume discharging from Smoke-and-Mirrors (S & M) hydrothermal edifice.

On the long-term end of the time scale (intervals of months to years), we anticipate detecting variations in hydrothermal flux due to (1) earthquake/faulting induced changes of permeability along flow paths (days), and (2) emplacement and cooling of magma bodies (decades). Earthquakes are likely to lead to changes in hydrothermal discharge rates and temperatures

(Johnson *et al.*, 2000). Both earthquakes and intrusions may induce microbial blooms (Delaney *et al.*, 1998). Local intrusions can initiate chemical and thermal cycles (e.g., Von Damm, 1995). The Endeavour segment is very active seismically producing hundreds of earthquakes per year up to a magnitude 4 (Fox *et al.*, 2001; Wilcock *et al.* 2002; Wilcock, 2004). Wilcock and Fisher (2004) comment that by monitoring seismicity and hydrothermal discharge, it may be possible to detect seismic events that perturb the system, yielding information about the geometry of the sub-seafloor flow. These studies so far indicate that the correlation distance between variations of hydrothermal flow and geologic events is plate-wide, meaning that earthquakes and volcanic events occurring anywhere on the Juan de Fuca plate can influence hydrothermal flow at a monitoring site.

Selection of a vent cluster to monitor depends on location with reference to the NEPTUNE Canada junction box (Figure 1), status of venting activity, and coordination with sensors to be emplaced by other investigators (to be determined). The COVIS is designed with a coil of 125 m of cable, which will give it flexibility to connect from the junction box to a suitable vent cluster. Conditions for a suitable vent cluster for monitoring by COVIS are location within range of the junction box (125 m), ongoing plume and diffuse flow, and coordination with other remote (e.g., acoustic scintillation, seismicity) and *in situ* sensors (temperature, chemistry, resistivity, camera imagery, current meter, etc.) from other investigators (to the extent feasible) in order to maximize the scientific return.

Our overall scientific objective is to utilize these data to determine the variability of hydrothermal fluxes from plume and diffuse flow and to elucidate linkages with oceanic and geological external forcing fields on time scales from hours to years. The operation of the sonar is planned for an initial period of five years. This temporal extension in coordination with observations of other investigators will enable acquisition of data to test scientific hypotheses with reference to seafloor hydrothermal flow with broad implications on scales ranging from vent clusters to tectonic plates.

- Different types of oceanic and geologic external forcing fields on time scales from hours to years provoke different responses in hydrothermal flow diagnostic of the forcing field. Earthquakes cause abrupt changes in circulation pathways of hydrothermal flow, which are expressed as perturbations in volume and heat flux and solution chemistry. Emplacement and cooling of magma bodies causes initial increase and gradual decrease of volume and heat flux of hydrothermal flow in conjunction with changes in fluid chemistry and microbial blooms.
- Fluctuating rather than “steady state” long term hydrothermal flow will influence thermal and other fluxes to the ocean.
- The correlation distance between geologic events and variations in hydrothermal flow (volume flux, heat flux, distribution of vents) is plate-wide, meaning that earthquakes and volcanic events occurring anywhere on the Juan de Fuca plate can influence hydrothermal flow at the monitoring site.
- The partitioning between plume and diffuse flow at a vent cluster is sensitive to external forcing fields with impacts on the vent ecosystem. Implementation of COVIS will open high-priority scientific opportunities for the community.

Acoustic Methods to Measure Seafloor Hydrothermal Flow

Acoustic Imaging of Hydrothermal Plumes

We use acoustic backscatter methods to volumetrically image (Rona *et al.*, 2002a; Bemis *et al.*, 2002) and Doppler methods to measure flow rates (Jackson *et al.*, 2003) in the initial tens of meters of turbulent rise of the buoyant plume, where mixing and reactions are most dynamic. Acoustic backscatter from hydrothermal plumes can be attributed to scattering by suspended metallic mineral particles, turbulent particle concentration fluctuations and/or turbulent

temperature (density) fluctuations. In our acoustic imaging work, the imaged plumes behave as if Rayleigh scattering from the particles, precipitated from high temperature hydrothermal solutions, dominates scattering in the spatial range acoustically imaged (*Palmer, 1996*). The particles are small (microns) relative to the wavelength of the acoustic frequencies used (~ 1 cm at 200 to 330 kHz). At sufficiently low particle concentrations (such that no acoustic self-shadowing of the plume or other multi-scattering effects occur) backscatter intensity is directly proportional to concentration of suspended particulate matter as the product of total particle load and a factor dependent upon average particle mechanical properties (density, bulk modulus, and radius; *Palmer, 1996; Palmer and Rona, 2005*).

Our VIP (Vent Imaging Pacific) 2000 experiment in the Main Endeavour Field used a commercial sonar system (Kongsberg Simrad Mesotech SM 2000) operating at 200 kHz and mounted on the tethered remotely operated vehicle ROV *Jason*. Acoustic data were recorded from a fixed position on the seafloor at a range of 10 to 20 m from a vent cluster. The 3D images are formed by means of a combination of time gating (for resolution in range), digital beam forming (for resolution in azimuth), and mechanical scanning (for resolution in elevation or height in the plume).

We reconstruct a plume by resampling the acoustic cross-section data onto a 3D rectangular grid (0.25 to 1 m spacing), averaging over as many scans as are available (typically, 6). The averaged data are converted to differential scattering cross section per unit volume. The averaged, gridded data are displayed as 3-D isointensity surfaces using standard visualization software (Figure 2, left panel).

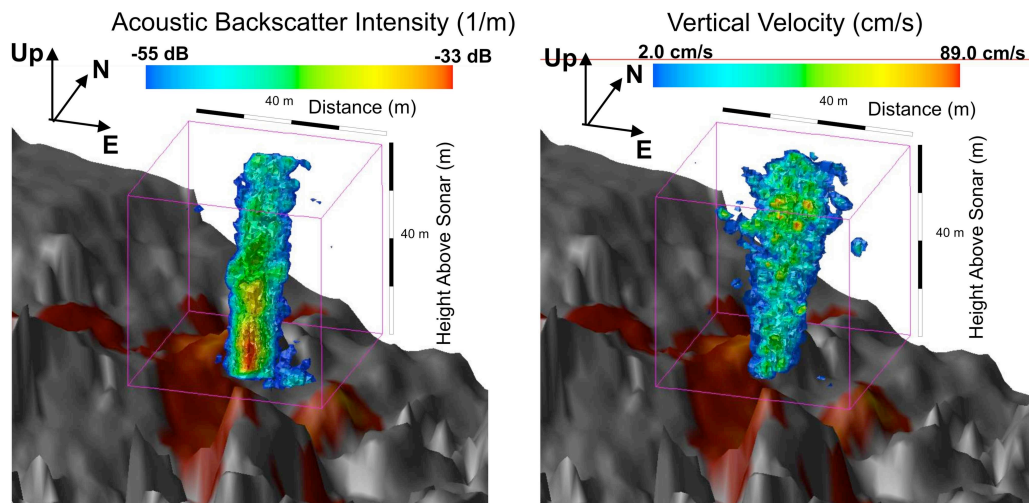


Figure 2. Left panel shows our acoustic image from the initial 40 m of rise of the buoyant stem of a major hydrothermal plume discharging from Grotto Vent in the Main Endeavour Field and the surrounding diffuse flow (red) draped over the seafloor bathymetry. Right panel shows isovelocity contours from the rising buoyant stem of the Grotto plume with the diffuse flow draped over the seafloor bathymetry (*Jackson et al., 2003*).

<http://geology.rutgers.edu/~bemis/AcousticImaging/acousticimagedraped.htm>

Scalar properties (including radius, connectivity of constituent objects, and bending) provide the basis to quantitatively compare the behavior of different hydrothermal plumes (*Bemis et al., 2002; Rona et al., 2002b*) and to assess entrainment rates and styles, especially as they relate to interaction between plumes and with the surrounding environment (*Bemis et al., 2002; Bemis and Rona, 2006; Rona et al., 2006*).

As part of our VIP (Vent Imaging and Processing) 2000 cruise, we acoustically imaged the main buoyant plume at Grotto Vent in the Main Endeavour Field hourly for 24 hours to determine the effect of the prevalent mixed semidiurnal tidal cycle on the plume (Figure 3). We observed that

maximum bending of the plume coincided with tidal highs and lows and that entrainment rate (0.07 to 0.18), indicated by rate of expansion of the plume with height, varied directly with degree of bending, showing a direct relation of entrainment to tidal forcing (Rona *et al.*, 2006). The lower values correspond to slack tide conditions and are similar to laboratory measured entrainment rates. A much longer time series (months), like that provided by a cabled observatory such as the NEPTUNE Canada RCO, is needed to unambiguously sort out these relations.

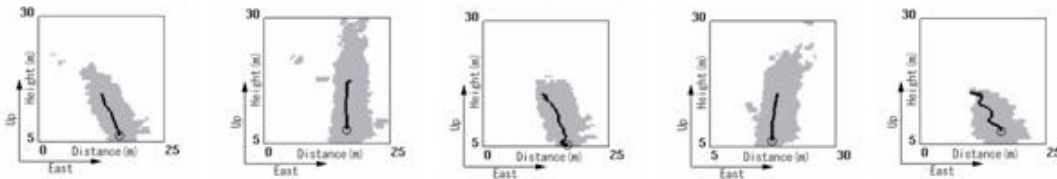


Figure 3. Five acoustic images (looking north) from our 23-hour time series imaging the initial 25 m of rise of the buoyant stem of the Grotto plume show the plume centerline (near-vertical black line) alternately bending to the southwest and to the northeast in apparent response to forcing by reversals in the mixed semi-diurnal tidal cycle (Rona *et al.*, 2006).

We have developed Doppler algorithms to measure mean vertical velocity at different altitudes in a plume (Jackson *et al.*, 2003). As the sonar can only measure velocity along the direction of the line of sight, a simple geometric correction is made to obtain vertical velocity based on the assumption that the net velocity is vertical. The vertical velocity image of the main Grotto plume was obtained from one sonar scan and shows complex structure (Figure 2, right panel). In effect, this is a snapshot. In this example, peak velocities of 30-40 cm/s are seen at altitudes to 30 m above the vent and a volume flux of 5.5 m³/s, +/- 0.4 m³/s at a height of 16 m above the vent (Jackson *et al.*, 2003). The flow velocity values are consistent with those obtained by the University of Washington Flow Mow group, which directly measured vertical accelerations by tracking motions of the autonomous benthic vehicle ABE as it flew over the Grotto plume (Viers *et al.*, 2006).

Acoustic Imaging of Diffuse Hydrothermal Discharge

We have developed and applied the Acoustic Scintillation Thermography (AST) method to detect and map diffuse flow in seafloor hydrothermal fields (Rona *et al.*, 1997). The AST method uses the phase-coherent correlation of acoustic backscatter from consecutive sonar scans of the seafloor to detect weak fluctuation in the index of refraction near the seafloor. The index of refraction changes result from temporal variations in the water temperature caused by turbulent mixing, which create detectable changes in travel time of an acoustic ray as the ray propagates from an acoustic transducer through the diffuse flow to the seafloor and is scattered back through the diffuse flow making the seafloor appear to shimmer. If the turbulent volume is assumed to be concentrated near the seafloor, then the de-correlation intensity is a measure of the temperature and velocity fluctuations in the near bottom boundary layer, providing a sensitive detection tool for mapping areas of flow (Jones *et al.*, 2000). We used the AST method from a fixed position on the seafloor to map the area of diffuse flow surrounding the Grotto plume on our VIP 2000 cruise (Figure 4). When the acoustic map is used in concert with *in situ* measurement of temperature and vertical flow velocity in the diffuse flow, heat flux can be calculated. For example, H. P. Johnson *et al.* (2002) subsequently applied the AST method using a ROV in a stop/start hovering mode to map the diffuse flow over a 3500 m x 900 m area of the Endeavour Segment axial valley. Using *in situ* sensors to simultaneously measure temperature and flow velocity, they calculated a diffuse heat flux of 150 MW integrated over the areas of the AST anomalies (Johnson *et al.*, 2002).

Acoustic Imaging Experimental Design and Observing Requirements

We will sequentially acoustically image buoyant plumes and associated diffuse flow on the scale of a vent cluster (dimensions tens of meters) using a single sonar instrument mounted on a tower

emplaced on the seafloor and operated in the plume and diffuse flow imaging modes, as we did successfully on our VIP 2000 experiment (Figures 2 and 3). The location of the sonar will be coordinated with that of *in situ* sensors emplaced by other investigators and with the position of a junction box emplaced by NEPTUNE Canada (Figure 1). The plume mode (Figure 2) comprises measurement of acoustic backscatter cross-section per unit of plume volume and Doppler measurement of flow velocity. The diffuse flow mode (Figure 4) is an application of the AST method. The specifications for a sonar position based on scientific requirements follow:

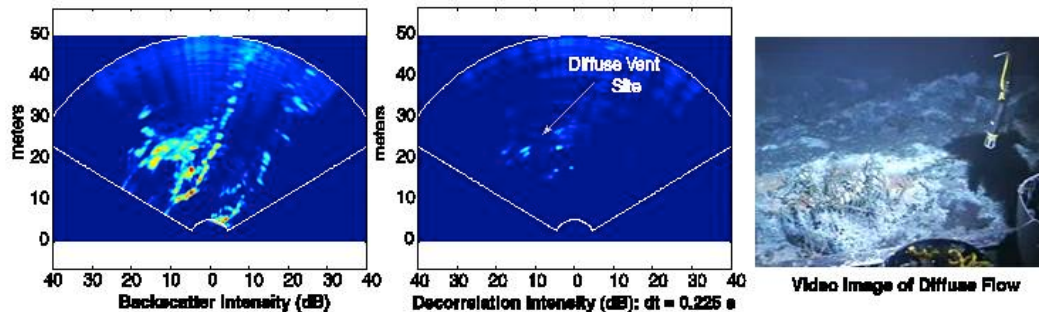


Figure 4. Sonar scans (120°) showing an AST image of diffuse flow near Hulk vent in the Main Endeavour Field (middle panel), a backscatter image of the same area (left panel), and a video image of the same area (right panel; Jones et al., 2000).

Horizontal position: A stationary point about 20 m west or northwest of the vents to be imaged (water depth ~ 2200 m), as close as feasible to orthogonal to the NE-SW excursion of the plume, as observed during the prevalent mixed semi-diurnal tidal cycle (Figure 3; Rona et al., 2006).

Vertical position: The sonar will be mounted on a fixed frame 5 m above the seafloor. In our VIP 2000 measurements, the sonar was at a water depth of 2187 m, oriented northeastward at a nearly horizontal slant range of 20 m to the vents on top of the Grotto edifice at a water depth of 2185 m. Thus the sonar had a nearly horizontal line-of-sight to the vents. We plan a lower placement, to obtain moderately steep upward-looking angles ($\sim 15^\circ$ to the base of the plume) to reduce the geometric correction of the measured line-of-sight velocity component to obtain the vertical flow rate.

Line of sight: 1) Plume imaging needs a clear line-of-sight from the sonar to within 1 m (vertical) of the vent orifice and higher portions of the plume. 2) Diffuse flow imaging needs a downward looking (c. 15° at 20 m range) line of sight view from a height of about 5 m above the area of diffuse flow. If the sonar has a vertical beamwidth of 25° it will cover horizontal ranges of roughly 10 m to 100 m at the level of the seafloor.

Cabled Observatory Imaging Sonar System (COVIS) Instrument Design

The COVIS instrumentation for the acoustic imaging of plume and diffuse flow back-scattering observations at hydrothermal vents, is designed for use on the deep ocean cabled observatory of NEPTUNE Canada and thus follows the NEPTUNE Canada Stage I functional requirements. Generally, instruments must be designed for continuous use and must respond to a status inquiry from the observatory at all times, shall automatically start up when connected, shall return to a known state when de-powered and re-powered, and shall use efficient power supplies. Communications between the instrument and the junction box must use the IEEE 802.3 Ethernet and be compatible with the TCP/IP family of protocols.

The acoustic instrumentation is capable of a broad range of acoustic imaging of various hydrothermal vent flows from plumes to diffuse flow producing high resolution spatial plume mapping and Doppler measurements of flow rates. The instrumentation was designed and fabricated by staff in the Ocean Engineering department of the Applied Physics Laboratory at the University of Washington (APL-UW). This department consists of professional engineers in

mechanical, electrical, and software engineering disciplines exclusively focused on ocean instrumentation. An extensive in-house machine shop and field engineering staff provide all the capability for fabrication, assembly, and at-sea operations. Other facilities include an Acoustic Test Facility at a nearby waterway, which includes annually leased Navy acoustic reference transducers for complete test and calibration of acoustic systems.

Sonar

The sonar is derived from a commercial-off-the-shelf (COTS) system from Reson, Inc., a 6000 m depth rating variant of the Seabat 7125. This state of the art imaging sonar represents a breakthrough in performance with unparalleled resolution and flexibility. The 400-kHz receiver unit provides 256, .5° horizontal beams and the corresponding transmitter unit provides a beam pattern of 128° (horizontal) x 1° (vertical) resulting in 256 beams with a resolution of .5° x 1°. Also offered is a 200-kHz receiver unit that provides 128, 1° (horizontal) beams but the corresponding transmitter unit has a 2° vertical beamwidth which would give poor vertical resolution in plume imaging. The better resolution in both the vertical and horizontal planes makes the 400-kHz system preferable. Each receive channel has a 35-kHz channel bandwidth for very high resolution.

A second projector will be used for diffuse flow imaging which provides a 128° (horizontal) x 28° (vertical) beam pattern. The receiver and projector sidelobe levels are very low, such that the net sidelobe power when imaging a diffuse target such as a plume is about 20 dB below the main lobe power. Update rates up to 50 Hz are possible. All raw data are available, which is required for image and Doppler data analysis. DC power and Ethernet interface are standard, which makes for easy integration with the cabled observatory system. The sonar used in previous experiments, the Simrad SM2000, is at the end of life having been designed more than a decade ago. It uses a proprietary telemetry system instead of Ethernet TCP/IP protocols, has a history of difficulty in developing customized software interfaces, much higher power rating >200 W, less resolution with fixed frequency operation of 200 kHz, and has passed through three different companies since its development (Mesotech, Simrad, Kongsberg). The Seabat 7125 offers improved performance in every aspect and is a new product.

Instrumentation for NEPTUNE Canada presents a challenging problem for developers in terms of long-term support, obsolescence, and reliability. It is essential when specifying COTS components to use new and stable components due to the longevity envisioned for the system. Reson is a stable company with a long track record in advanced sonar products and will be an excellent partner for the duration of the NEPTUNE Canada system. A review of potential sonar systems for the COVIS application indicated that the Reson Seabat 7125 meets all systems requirements. An NSF-funded sonar developed by Dr. Chris Jones (APL-UW) was considered for this application, but was rejected because it is untested and unsupported.

General Characteristics

The COVIS consists of a benthic tripod base lander with a central tower. At the top of the tower is a 3-degree of freedom rotational system, which will allow the sonar transducer elements to be aimed in a nearly unlimited number of directions (Figure 5). Three independent motors with positional feedback will provide $\pm 170^\circ$ travel in pitch, roll, and yaw (pan). Each motor will be installed in oil filled, pressure balanced cases to simplify seal design and improve reliability. Each motor has a high accuracy, absolute angular position sensor that provides feedback to the motor controller for positioning control and observational data. The rotational system simplifies the installation of the COVIS in the unknown topography of the experimental site. It is critical to position the plume imaging fan beam orthogonal to the plume flow and then to quickly image the flow in 1 degree increments through a 60° range. Unknowns in the bottom topography, edifice height, plume location and diffuse flow locations are alleviated through this rotational system. A high accuracy pitch/roll/magnetic compass sensor will be installed on the sonar head assembly for independent verification of the sonar position and to provide geo-referenced datum for sonar data.

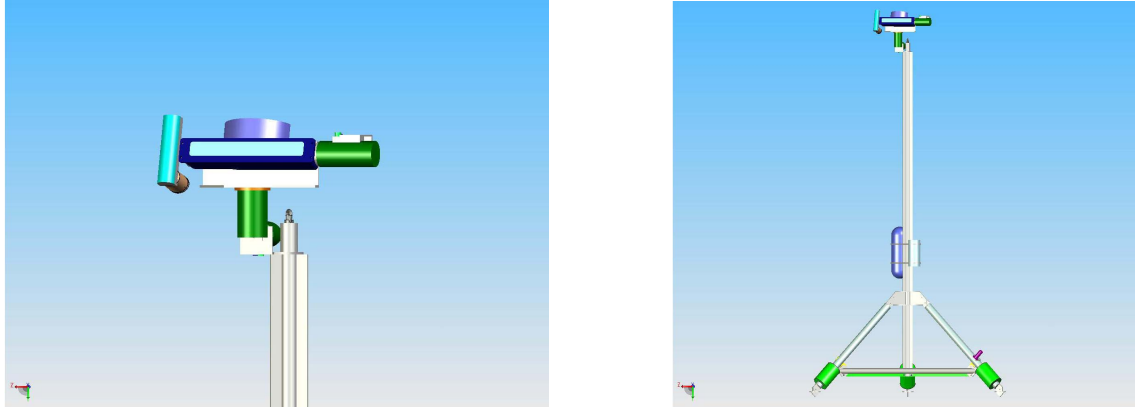


Figure 5. (Left) COVIS sonar transducer assembly concept and (right) COVIS tower concept.

Electrical Design

An Interface Computer (IC) is used to orchestrate the Reson sonar, the angular translation system, and the sonar head attitude sensor. The IC provides flexibility in dealing with the sonar software interface issues and the observatory network protocols as well as providing control to the translation system, the attitude sensor, and potentially interfacing to future sensors (e.g., vent temperature sensor). Figure 6 is a wiring diagram of the system. The IC electronics make use of COTS hardware based around the PC-104+ bus architecture (see Figure 6).

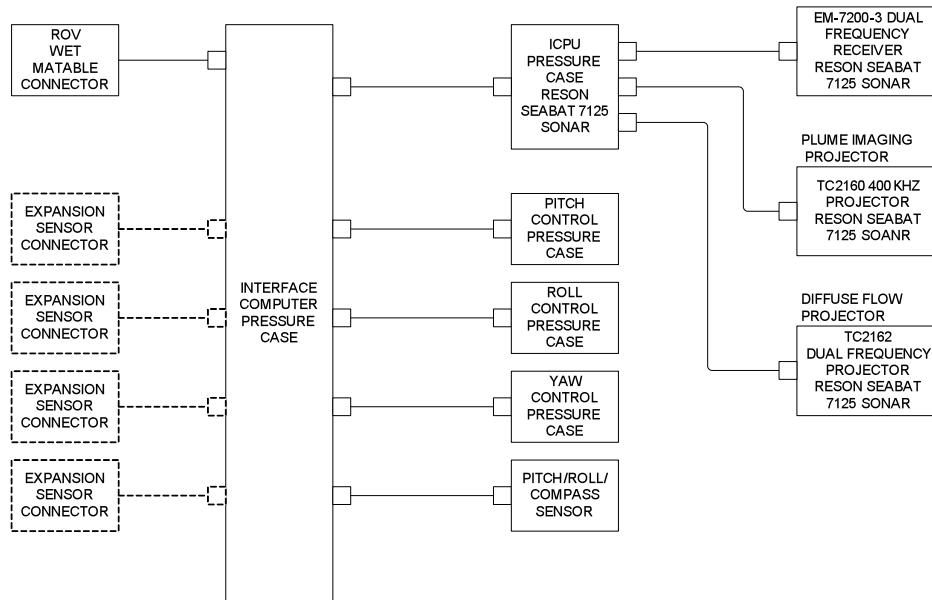


Figure 6. COVIS system level wiring diagram

Custom interfacing hardware such as power or signal conditioning is located in this case. The CPU board runs a Windows or Linux operating system providing networking capability to an application that controls the angular translation system, sensor signal acquisition, and sonar control. A flash memory disk drive provides a temporary sonar data storage area before moving the data to the shore based archive. This decouples observatory bandwidth from experimental sonar operation. A relay control board allows power switching of each motor and sensor. This will improve reliability in the case where a cable or connector fails resulting in a short to seawater of the motor or sensor power supply. Depending on the failure, some experimental operations may be continued with the loss of part of the system.

Media converter (fiber to copper) cases are built into the ends of the interconnect cables. Short

copper cables (2-3m) with ROV mateable connectors extend out of the media converter cases to connect to mating connectors at the junction box and COVIS. In addition, concern over COVIS recovery led to the determination that the system needs ROV mateable connectors at both the COVIS and the junction box (this is standard at the junction box). Seabed topology in the MEF can be extremely rugged and it may not be possible for the ROV to disentangle the interconnect cable during instrument recovery. ROV mateable connectors at both ends allows for greater flexibility in both installation cable laying, recovery of the COVIS and recovery of the interconnect cable.

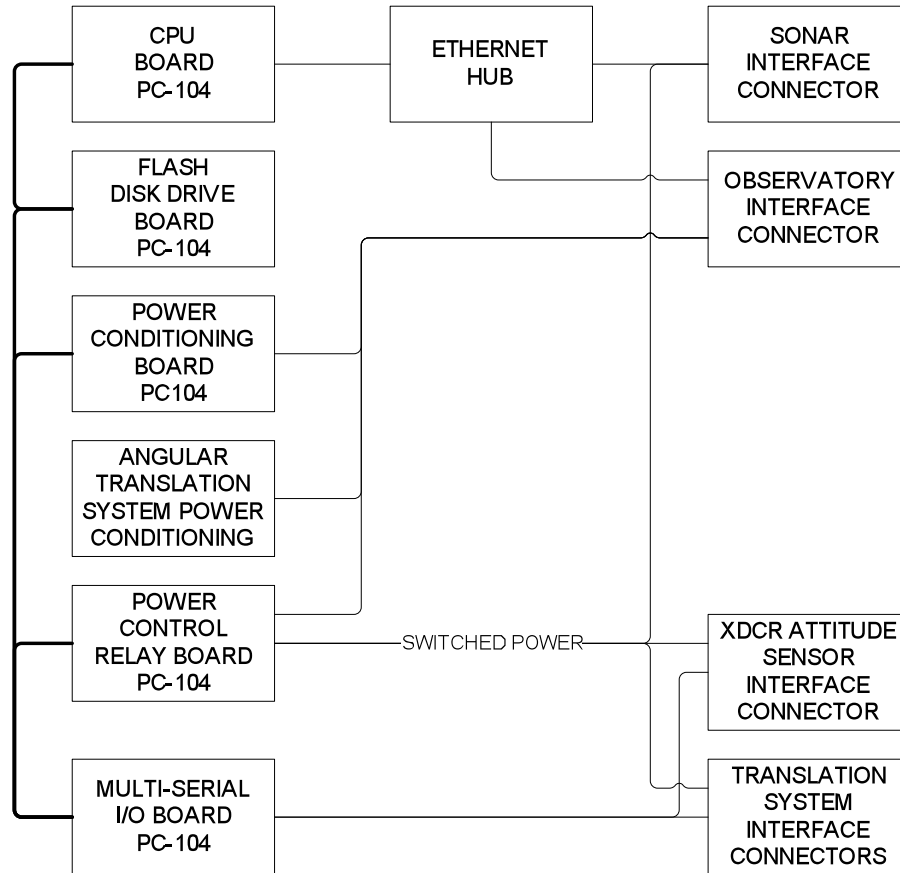


Figure 7. COVIS interface computer simplified block diagram

Mechanical Design

The COVIS tower (Figure 5) is a 5-m-tall tubular and plate structure that provides a stable platform for mounting the sonar and electronic pressure cases. The base of the tower is 2.5 m between footpads requiring a minimum of a 2.5 m square area on the seafloor. The tower's tripod design allows deployment on rough ground and its low center of gravity allows placement on slopes up to 20 degrees. The structural frame is constructed entirely from titanium to minimize corrosion problems while operating for multi-year periods in the hydrothermal field environment. Lead ballast rings are mounted on each tower leg to trim the tower as required for a low center of gravity and spiked feet are added to minimize slipping of the tower on rock slopes. The tower will weigh approximately 680 kg (in water) and is designed to be deployed and recovered by the ROPOS ROV using the through frame lift capability.

Lifting and handling of the tower is done with a single eye bolt located at the top of the tower mast. A 3-m long lifting strap is permanently attached to this eye bolt. A ship's crane hook may be attached to the end of this strap for lifting the tower. During deployment and recovery of the tower, the lift strap is secured to the ROPOS's frame lift line. Electrical connection to the tower is

made through a ROV underwater mateable electrical connector, which is located on one of the legs, at the base of the tower. The 125-m junction box interface cable is stored on the tower.

After placement of the COVIS at the desired site the cable is pulled off the tower by ROV and laid over the seabed to the NEPTUNE Canada junction box. Periodic, breakable restraints are used to hold the cable to the tower during deployment but will release easily with the pull from the ROV. The Reson ICPU and the APL-UW IC electronic cases are mounted on the tower mast immediately above the apex of the tower legs. Both of these electronic cases are constructed from titanium. The electrical cables connecting the electronics housings to the sonar head are routed up the length of the mast along the mast valleys to provide mechanical protection. At the mast head, each electrical cable is secured in a fashion that will minimize cable wear or snagging while the sonar head rotates. After the tower is deployed and the sonar head is rotated to face the sulfide edifice, the dominant motion of the sonar head will be pitch as the head scans between lower and upper regions of the plume. Underwater electrical cables will be chosen for maximum flexibility to minimize the wire fatigue during this pitch motion.

Plume Imaging Concept

Figure 8 is a conceptual scale drawing of the COVIS installed ~20 m from a typical hydrothermal edifice. The height of the COVIS tower provides good acoustic coverage of the vent plume at this range and edifice height and allows deployment by a typical surface ship's A-frame and boom crane equipment.

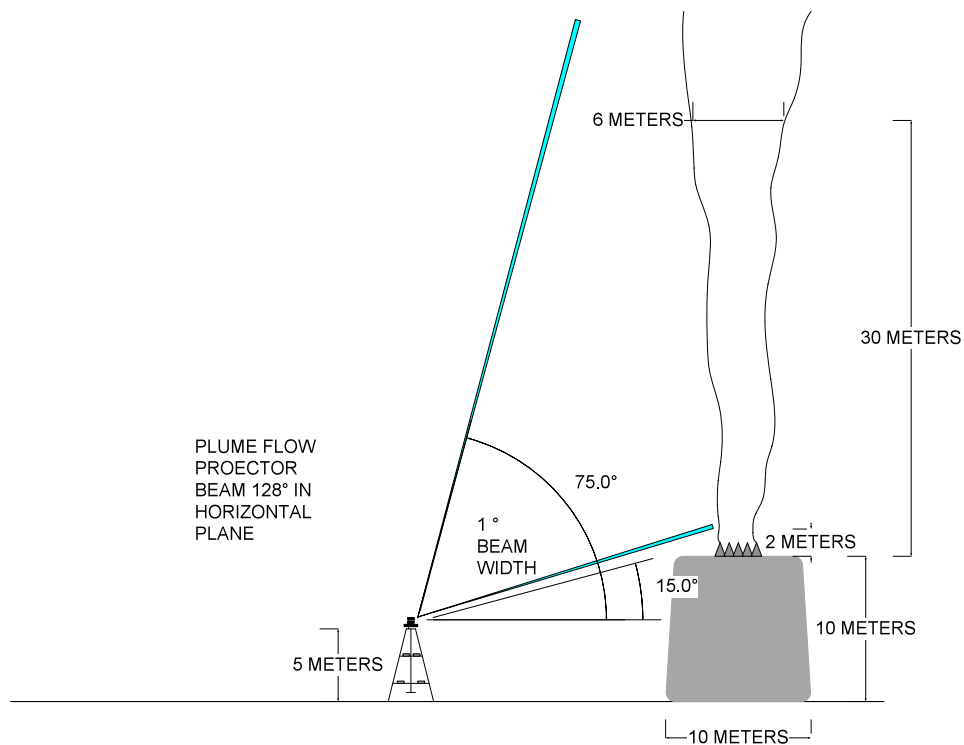


Figure 8. Approximate scale drawing of plume imaging concept.

Diffuse Flow Imaging Concept

For diffuse flow imaging the wider 28° vertical beam acoustic projector is used. Shown in Figure 9 the COVIS can image most of a typical sulfide edifice with a single transmission at a zero degree pitch angle. The angular translation system allows diffuse flow imaging of the edifice base and surrounding areas.

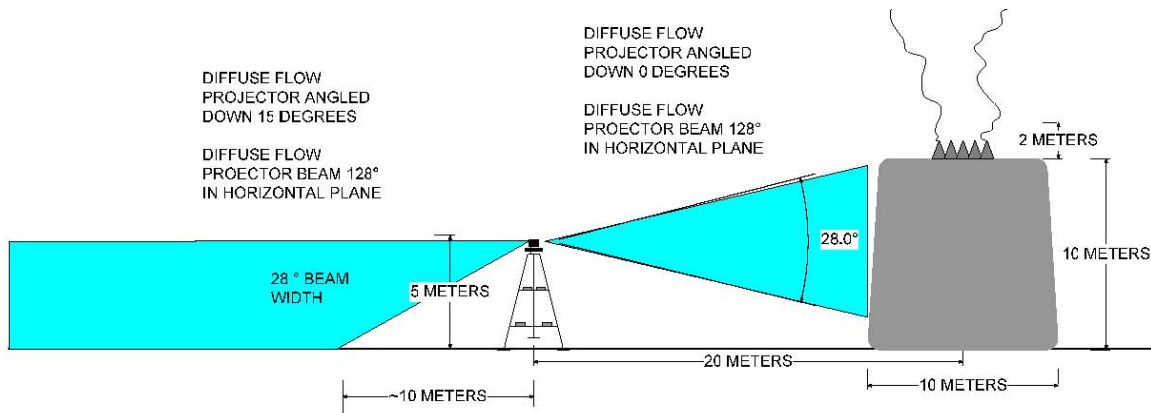


Figure 9. Approximate scale drawing of diffuse flow imaging concept.

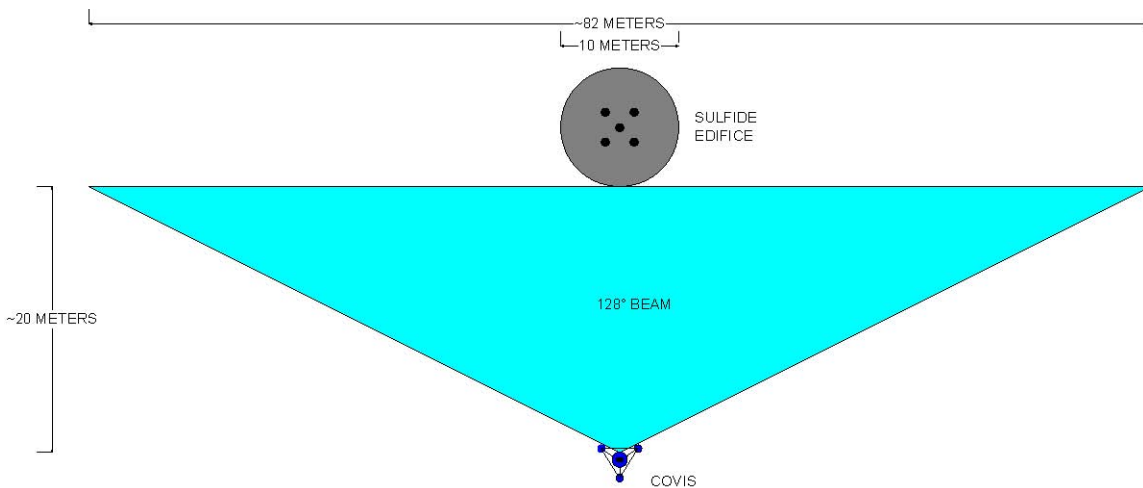


Figure 10. Approximate scale drawing of top view for plume or diffuse flow imaging.

Software Design

The RESON Seabat sonar is designed around TCP/IP and UDP protocols over 100BaseTX Ethernet and thus is ideally suited for the NEPTUNE Canada Stage I system. The NEPTUNE Canada Data Management and Archival System (DMAS) places a number of requirements upon instrument software (NEPTUNE STAGE I FUNCTIONAL REQUIREMENTS INSTRUMENTS, ISSUE 1.7 APRIL 28, 2006). For initial deployment, APL-UW and Rutgers engineers will need direct control over COVIS using a combination of custom developed application software and Reson COTS software. DMAS specifications allow for this type of direct control for complex instruments though over time it is envisioned that control will occur via DMAS software agents. The Interface Computer and internal Ethernet hub provide for the ability to operate the COVIS in a direct mode where all commands and data packets pass through the entire observatory network or in a batch mode, high-level fashion. The direct mode will allow the use of Reson COTS software, direct control over the IC and Reson operating systems, and updating of system software. A shore-based application orchestrates the angular translation system and sonar to perform high level experiments such as the complete activity of plume imaging.

Initially the instrument will be run using this software in direct mode to the instrument. This code will form the basis for another application, which will run on the IC to perform high level experiments without observatory network activity. This allows the COVIS to operate at maximum efficiency since all sonar and translation system activity is local to the instrument and the network latencies are eliminated. In addition, this application will provide a simple interface for DMAS

control once the system has matured.

A critical element to the NEPTUNE system is synergistic operation of observatory instruments. It is envisioned that DMAS software agents will autonomously monitor quick look data products from observatory instruments. When programmed conditions are detected, observatory instruments will be directed to special sampling scripts. An example would be a significant seismic event. COVIS could be autonomously directed to run a script that would increase its rate of plume and diffuse flow imaging in response to a special event regardless of the time or level of human monitoring.

Data and Power Requirements

The Reson sonar collects data at a rate of ~18 kb/ms when using 200 kHz. Table 1 provides the data amounts for the (3) experimental modes of operation: plume imaging, plume Doppler, and diffuse flow. Both 200-kHz and 400-kHz sonar frequencies are provided as the Reson sonar can support both (the current projector only works at either 200 kHz or 400 kHz, a unit under development can provide both frequencies, the receiver supports both now).

Table 1. Data amounts for COVIS experimental modes

TYPICAL EXPERIMENT			
PLUME IMAGING (pulse length <.5mS)		PLUME DOPPLER (pulse length > 1mS)	
No of xmit per elevation	2 xmits	No of xmit per elevation	10 xmits
Elevation range	60 degrees	Elevation range	60 degrees
Elevation increment	1 degrees	Elevation increment	1 degrees
Total no. of xmits	120 xmits	Total no. of xmits	600 xmits
Typ Repeat Count	4	Typ Repeat Count	1
Total Data Amount (400khz)	1357 Mbytes	Total Data Amount (400khz)	1696 Mbytes
Total Data Amount (200khz)	678 Mbytes	Total Data Amount (200khz)	848 Mbytes
DAILY OPERATION SCHEDULE		DIFFUSE FLOW	
Plume Image Rate	4 per day	No of xmit per elevation	5 xmits
Plume Doppler Rate	4 per day	Elevation range	1 degrees
Diffuse Flow Rate	4 per day	Elevation increment	1 degrees
		Total no. of xmits	5 xmits
Total Data Per Day	400khz	Typ Repeat Count	1
Plume Image Rate	5.43 Gbytes	Total Data Amount (400khz)	14 Mbytes
Plume Doppler Rate	6.78 Gbytes	Total Data Amount (200khz)	7 Mbytes
Diffuse Flow Rate	0.06 Gbytes		
Total	12.27 Gbytes		
	200khz		
Plume Image Rate	2.71 Gbytes		
Plume Doppler Rate	3.39 Gbytes		
Diffuse Flow Rate	0.03 Gbytes		
Total	6.13 Gbytes		

Assumes a sonar digitization period of 80 ms, or 60-m target range.

Table 2 describes the approximate power usage for the COVIS systems. The Reson and IC system are on continuously when power is applied to the system.

Rotator motors will only be used during experimental operations. Only one motor will be run at a time. During an experimental cycle a motor will be running almost continuously. Sonar data will be taken rapidly and for plume imaging the pitch angle will be moving in 1° increments. It is expected that the translation system can achieve 1° movements in 1 second. In Table 3 a conservative estimate for the time to complete each of the experiments in Table 1 is given.

Table 2. COVIS power requirements

COVIS Sub-System	Avg Power (W)	Peak Power (W)
Reson Seabat 7125	90	120
Interface Computer	10	15
Rotator Motor	24	24
TOTAL	124	159

Table 3. COVIS estimated experiment times

COVIS Experiment	Time (minutes)
Plume Image ¹	5.9
Plume Doppler ¹	13.6
Diffuse Flow ²	2

¹Assumes rotator moves 1°/sec, 60° of elevation repeated 4 times, sonar data acquisition overhead is equal to 3 times the time of sonar digitization

²Assumes rotator moves 1°/sec, pan motor moves 90°, roll motor moves 10°, pitch motor moves 15°

Instrument Maintenance

There are four areas of concern for COVIS maintenance: corrosion, biofouling, rotator seal wear, and transducer assembly cable fatigue. The issue of corrosion has been addressed by the use of titanium for all components wherever possible. The Reson sonar transducer housings are constructed from titanium. Biofouling of the acoustic transducer faces can degrade sonar performance if severe. A yearly brushing of the transducer faces by ROV should suffice to keep these areas clear. The 5 m COVIS tower height also reduces the possibility of biofouling these areas since they will be well clear of the thermophilic organisms. Instruments deployed for 6 weeks at the study site came up clean (D. Di Iorio, pers. comm.)

Rotator seal wear will be minimized through the use of judicious system operation. A COTS rotator motor was identified as a candidate for implementation of the 3 degree of freedom angular translation system. Three motors from Remote Ocean Sensing (ROS), Model R-25-FB, will meet the system requirements. It is recognized that these rotator motors present a long-term reliability issue. ROS's experience with rotational shaft motors in ocean environments have led to a robust design using an oil filled, pressure balance case. This allows the shaft seal o-ring to be maintained in a relaxed state as the pressure is equal on both sides of the seal. The o-rings and quadseals used in these motors are made from Buna N material that has been shown to have an operational life of 5 years (from the manufacturer Parker) and 10 years from military testing (source ROS). Seawater and mineral oil are very compatible with the Buna N material. The gears used in the rotators are rated for continuous use with an input speed of 3500 RPM but will only be run around 266 RPM, which significantly reduces wear. The immersion of the gears in mineral oil provides ideal lubrication. ROS has never seen a gear failure in over 30 years in the R25 unit. ROS has noted problems with the motor controller electronics from repeated pressure cycling such as use on an ROV. The COVIS system is designed for long-term deployment and therefore should not see undue stress on the electronics in the pressure balanced case.

The electrical cables to the transducer head will undergo movement during transducer assembly positioning. Careful cable routing, cable selection, and judicious system operation will minimize cable fatigue.

Data Acquisition, Management and Assessment

The NEPTUNE Canada Data Management and Archiving System (DMAS) provides basic data services for COVIS as with the majority of instruments connecting to the observatory. In

particular, DMAS downloads the raw data from the instrument to the shore station, archives data products and possibly raw data, and provides access to data products. The raw data are archived at least until released on the basis of partial reprocessing and reassessment of quality control; longer term storage depends on data quality, usage and demand.

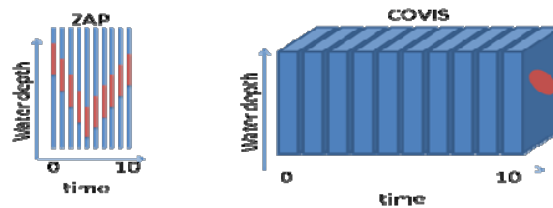


Figure 11. Contrasting data rates and dimensions of VENUS's ZAP and COVIS for 10 time increments shows the greater data rates of COVIS and that it produces 3D volumes instead of 1D lines. The data point of interest is mostly hidden in this view of the volumes.

The COVIS instrument will provide a binary data file that comprises the raw acoustic signal. For simpler acoustic instruments (e.g., single hydrophone or an ocean-bottom seismometer), the raw signal can be plotted as a single magnitude; for COVIS, the equivalent is a 3D array – that is, a full 3D volume of data is collected during each imaging session (as a series of 2D arrays, one for each pulse of sound emitted). In order to determine if there is a signal (such as a plume or a fish school), this data must be visualized into an image that conveys the 3D relationships and distribution of magnitudes of backscatter. Compare the Zooplankton Acoustic Profiler (ZAP) currently connected to the VENUS cabled observatory with the projected COVIS (Figure 11): (1) ZAP produces a line of data for each pulse whereas COVIS produces a 2D array for each pulse, (2) conceptually, ZAP images a vertical line in the ocean for each data acquisition instance whereas COVIS images a box (with contents) for each data acquisition instance, and (3) ZAP data can be easily summarized in a 2D diagram whereas the equivalent summary of COVIS data is a series of 3D volume images. Figure 11 conveys the difference in dimensions of ZAP and COVIS data.

Plotting a line of magnitudes so they can be seen is simple and leaves the burden of interpretation on the user. Plotting a 3D volume is more difficult as the front obscures the back (i.e., images are fundamentally 2D even for cameras!). Software must be created to convert the 3D volume of data to a 2D image – thus, the output of the COVIS instrument will be akin to that of a camera in that it is a series of images; however, significant processing is required to produce a 2D image from 3D acoustic data.

Processing steps include (1) electronic beam steering calculations on the raw signal to produce the actual spatial array of backscatter, (2) signal processing to remove noise and unwanted reflections from the seafloor and sulfide structures and to highlight the backscatter coming from the actively rising plume, (3) identification of a threshold indicative of plume signal, and (4) visualization algorithms such as ray tracing to create an interpretable image. Bemis, Rona, and Silver (RU team) have considerable experience producing images from acoustic volume data (Bemis *et al.*, 2002; Rona *et al.*, 2002). Preliminary software has been developed to produce images from streaming sonar data in near real-time (Dastur, 2005). This initial software does not include any signal processing so the image produced (see example in Figure 12) contains multiple artifacts as well as the true plume signal.

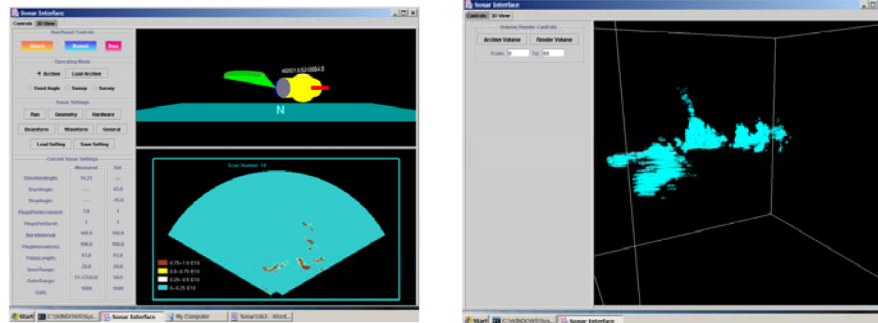


Figure 12. The two screen capture shots above show a sonar interface designed to stream real-time data into an archive, to visualize the data as it streams by in 2D slices, and to visualize data volumes as sufficient data is acquired. Of particular interest to this proposal is its 3D visualization capability as shown on the image to the right. The main plume is the narrow (but widening) ribbon above the seafloor.

We plan to implement conversion of preliminary real-time software (designed to utilize the rapid hardware processing capabilities of early NVIDIA video cards) to run on current computer hardware. We will also develop real-time signal processing capabilities to increase the quality of the produced images and develop data quality assessment algorithms to fulfill NEPTUNE Canada's request for data quality assessment, as well as assisting the user in determining the detail level in which to interpret the images. Further processing is necessary to produce parameters of direct geologic interest, such as entrainment rates and flow rates.

References

- Bemis, K., D. Silver, P. Rona, and J. Cowen, 2006, A particle sedimentation model of buoyant jets: observations of hydrothermal plumes, *Cahiers de Biologie Marine*, 47, 379-384.
- Bemis, K.G., D. Silver, P. Rona, and J. Cowen, 2005, A particle sedimentation model of buoyant jets: observations of hydrothermal plumes, *Eos Trans. AGU*, 86 (52), Fall Meet. Suppl., Abstract T31A-0484.
- Bemis, K.G., Deborah Silver, Peter Rona, 2004a, A particle sedimentation model of buoyant jets based on observations of hydrothermal plumes, *IUGG's Committee on Mathematical Geophysics, Frontiers of Theoretical Geophysics*, conference abstract.
- Bemis, K.G., P.A. Rona, K. Santilli, J. Dastur and D. Silver, 2004b, Inferences of particle size and composition from video-like images based on acoustic data: Grotto Plume, Main Endeavor Field, *EOS, Trans. AGU* (abstract).
- Bemis, K.G., P.A. Rona, D. Jackson, C. Jones, D. Silver, K. Mitsuzawa, 2002, A comparison of black smoker hydrothermal plume behavior at Monolith Vent and at Clam Acres vent field: dependence on source configuration, *Marine Geophys. Res.*, 23:81-96.
- Bemis, K. G., and Rona, P. A., 2006, Are hydrothermal plumes lazy?: implications for the entrainment of diffuse flow, *Eos Trans. AGU*, 87(52), *Fall Meet. Suppl.*, Abstract B33D-08.
- Crone, T.J., W.S.D. Wilcock, 2005, Modeling the effects of tidal loading on mid-ocean ridge hydrothermal systems, *Geochemistry Geophysics Geosystems* 6(7), Q07001, doi:10.1029/2004GC000905, ISSN:1525-2027.
- Dastur, J., 2005, A real time interface for visualization and control of an oceanographic sonar system, M.A. Thesis, Rutgers University.
- Delaney, J.R., D.S. Kelley, M.D. Lilley, D.A. Butterfield, J.A. Baross, W.S.D. Wilcock, R.W. Embley, and M. Summit, 1998, The quantum event of oceanic crustal accretion: Impacts of diking at mid-ocean ridges, *Science*, 281, 222-230
- Edmond, J.M., C. Measures, B. Mangum, B. Grant, F.R. Sclater, R. Collier, and A. Hudson, 1979, On the formation of metal-rich deposits at ridge crests, *Earth and Planetary Science Letters*, 46:19.
- Elderfield, H., and A. Schultz, 1996, Mid-ocean ridge hydrothermal fluxes and the chemical composition of the ocean, *Annual Reviews of Earth and Planetary Science*, 24, 191-224.
- Fox, C. G., H. Matsumoto, and T.-L. A. Lau, 2001, Monitoring Pacific ocean seismicity from an autonomous hydrophone array, *J. Geophys. Res.*, 106, 4183-4206.
- Garcia-Berdeal, I., S.L. Hautala, L.N. Thomas, and H.P. Johnson, 2006a, Vertical structure of time-dependent currents in a mid-ocean ridge axial valley, *Deep-Sea Research*, 1 53, 367-386.
- Garcia-Berdeal, I., S.L. , H.L.. Hautala, M.J. Pruis, and H.P. Johnson, 2006b, Diffuse hydrothermal venting into the turbulent bottom boundary layer on the Endeavour Segment, Juan de Fuca Ridge. II. Variability and implications for particle flux near the bottom, preprint submitted to Elsevier Science.
- Jackson, D.R., C.D. Jones, P.A. Rona and K.G. Bemis, 2003, A method for Doppler acoustic measurement of black smoker flow fields, *G-Cubed* , 4 (11), 1095. doi:10.1029/2003G000509, 1-12.
- Jenkins, W.J., J.M. Edmond, and J.B. Corliss, 1978, Excess ³He and ⁴He in Galapagos submarine hydrothermal waters, *Nature*, 272: 156-158.
- Johnson, H.P., S.L. Hautala, M.A. Tivey, C.D. Jones, J. Voigt, M. Pruis, I. Garcia-Berdeal, L.A. Gilbert, T. Bjorklund, W. Fredericks, J. Howland, M. Tsurumi, T. Kurakawa, K. Nakamura, K. O'Connell, L. Thomas, S. Bolton, and J. Turner, 2002, Survey studies hydrothermal circulation on the northern Juan de Fuca Ridge, *Eos, Trans. AGU*, 83, 73.
- Johnson, H.P., M. Hutnak, R.P. Dziak, C. Fox, I. Urcuyo, J.P. Cowen, J. Nabelek, and C. Fisher. 2000, Earthquake-induced changes in a hydrothermal system on the Juan de Fuca mid-ocean ridge. *Nature* 407: 174-177.
- Johnson, H.P., and M.J. Pruis, 2003, Fluxes of fluid and heat from the oceanic crustal reservoir, *Earth and Planetary Science Letters*, 216., 565-574.
- Jones, C.D., D.R. Jackson, P.A. Rona and K.G. Bemis, 2000, Acoustic observation of hydrothermal flow (abs.), *J. Acoust. Soc. Am.*, 108:5:Pt.2:2544-2545.
- Kim, S.L., L.S. Mullineaux, and K.R. Helfrich, 1994, *J. Geophysical Research*, 99(C6), 12,655-12, 665.
- Lilley, M.D., D.A. Butterfield, J.E. Lipton, and E.J. Olson, 2003, Magmatic events can produce rapid changes

- in hydrothermal vent chemistry, *Nature*, 422, 878-881.
- McDuff, R.E., 1995, Physical dynamics of deep-sea hydrothermal plumes, in *Seafloor Hydrothermal Systems: Physical, Chemical, Biological and Geological Interactions*, *Geophys. Monogr. 91*, edited by S.E. Humphris et al., 357-368, AGU, Washington, D.C.
- Morton, B. R., G.I Taylor, and J.S. Turner, 1956, Turbulent gravitational convection from maintained and instantaneous sources, *Proc. R. Soc London, Ser. A*, 234, 1-23.
- Mullineaux, L.S., P.H. Wiebe, and E.T. Baker, 1991, Hydrothermal vent plumes: larval highways in the deep sea?, *Oceanus*, 34, 64-68.
- Palmer, D. R., 1996, Rayleigh scattering from nonspherical particles, *J. Acoust. Soc. Am.* 99, 1901-1912.
- Palmer, D.R., and P.A. Rona, 2005, Acoustical imaging of deep ocean hydrothermal flows, invited chapter in H. Medwin (Editor), *Sounds in the Sea*, Cambridge University Press, 643 pp., 551-563.
- Pruis, M.J. and H.P. Johnson, 2004, Tapping into the sub-seafloor: examining diffuse flow and temperature from an active seamount on the Juan de Fuca Ridge, *Earth and Planetary Science Letters*, 217(3-4), 379-388.
- Rona, P.A., and D.A. Trivett, Discrete and diffuse heat transfer at ASHES vent field, Axial Volcano, Juan de Fuca Ridge, *Earth and Planetary Science Letters*, 109:57-71.
- Rona, P.A., D.R. Jackson, T. Wen, K. Mitsuzawa, C. Jones, K.G. Bemis, and J.G. Dworski, 1997, Acoustic mapping of diffuse flow at a seafloor hydrothermal site: Monolith Vent, Juan de Fuca Ridge, *Geophys. Res. Letters*, 24:2351-2354.
- Rona, P.A., K.G. Bemis, D. Silver and C.D. Jones, 2002a, Acoustic imaging, visualization, and quantification of buoyant hydrothermal plumes in the ocean, *Marine Geophys. Res.*, 23:147-168.
- Rona, P. A., D. R. Jackson, K.G. Bemis, C. D. Jones, K. Mitsuzawa, D. R. Palmer, and D. Silver, 2002b, Acoustics advances study of sea floor hydrothermal flow (feature article), *Eos, Trans. AGU*, 83(44): 497 & 501-502.
- Rona, P.A., K. G. Bemis, C. D. Jones, D. R. Jackson, K. Mitsuzawa, and D. Silver, 2006, Entrainment and bending in a major hydrothermal plume, Main Endeavour Field, Juan de Fuca Ridge, *Geophys. Res. Letters*, 33, L19313, doi:10.1029/2006GL027211.
- Santilli, K., K. Bemis, D. Silver, P. Rona, and J. Dastur, 2004, Generating realistic images from hydrothermal plume data, *IEEE Visualization 2004 Proceedings*, pp. 91-98.
- Schultz, A., Delaney, J., and McDuff, R., 1992. On the partitioning of heat flux between diffuse and point source seafloor venting, *J. Geophys. Res.*, 97(B9), pp 12299-12314.
- Turner, J.S., 1986, Turbulent entrainment : the development of the entrainment assumption, and its application to geophysical flows, *J. Fluid Mech.*, 173, 431-471.
- Viers, S. R., McDuff, R. E., and Stahr, F. R., 2006, Magnitude and variance of near-bottom horizontal heat flux at the Main Endeavour hydrothermal vent field. *Geochemistry, Geophysics, Geosystems G3*, 7(2), doi:10.1029/2005GC000952.
- Von Damm, K.L., 1995, Controls on the chemistry and temporal variability of seafloor hydrothermal fluids, in *Seafloor Hydrothermal Systems: Physical, Chemical, Biological and Geological Interactions*, *Geophys. Monogr. 91*, edited by S.E. Humphris et al., 222-247, AGU, Washington, D.C.
- Wilcock, W.S.D., 2004, Physical response of mid-ocean ridge hydrothermal systems to local earthquakes, *Geochemistry Geophysics Geosystems*, 5, Q11009, doi:10.1029/2004GC000701,2004.
- Wilcock, W. S. D., S. D. Archer, and G. M. Purdy, 2002, Microearthquakes on the Endeavour segment of the Juan de Fuca Ridge, *J. Geophys. Res.*, 2336, doi:10.1029/2001JB000505.
- Wilcock, W. and Fisher, A., 2004. Geophysical constraints on the sub-seafloor environment near midocean ridges, In *Subseafloor Biosphere at Mid-Ocean Ridges*, Wilcock, W., Cary, C., Delong, E., Kelley, D., and Baross, J., editors. American Geophysical Union, Washington DC.
- Wilcock, W.S.D., T.J. Crone and R.E. McDuff, 2003, Tidal variations in fluid discharge velocities at midocean Ridge hydrothermal systems: a critical measurement, *Geophysical Research Abstracts*, 5, 07121, European Geophysical Society.